Generation and diagnostics of pulsed intense ion beams with an energy density of 10 J/cm2

Yu. Isakova, A. Pushkarev, I. Khailov, and H. Zhong

Articles you may be interested in

Neutralization of space charge on high-current low-energy ion beam by low-energy electrons supplied from silicon based field emitter arrays
AIP Conf. Proc. **1496**, 368 (2012); 10.1063/1.4766565

Design and development of a radio frequency quadrupole linac postaccelerator for the Variable Energy Cyclotron Center rare ion beam project
Rev. Sci. Instrum. **81**, 023301 (2010); 10.1063/1.3280175

Measurements of transverse ion beam emittance generated by high current ion sources at the GSI test injector facility HOSTIa)
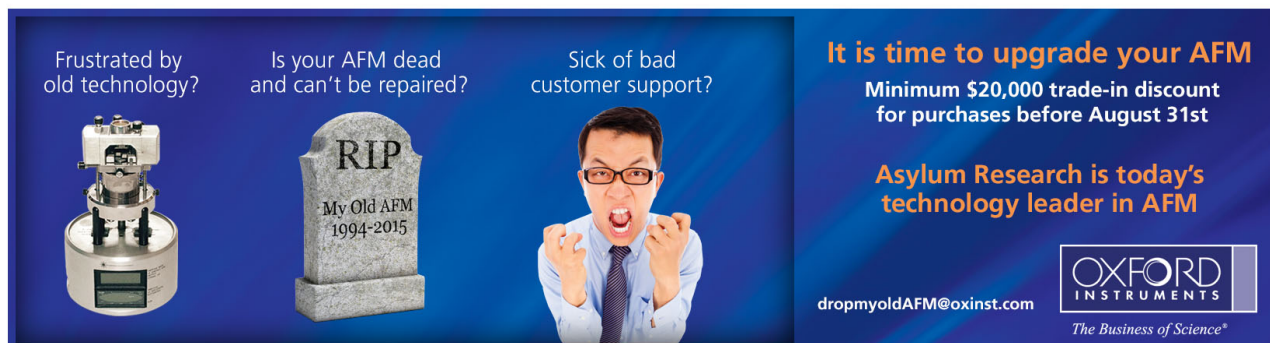Rev. Sci. Instrum. **81**, 02B707 (2010); 10.1063/1.3273066

Generation of intense beams of Pb +4 to Pb +10 ions in a laser ion source
Rev. Sci. Instrum. **73**, 1121 (2002); 10.1063/1.1448908

Time resolving diagnostic of the compensation process of pulsed ion beams at high-intensity light ion source
Rev. Sci. Instrum. **71**, 1107 (2000); 10.1063/1.1150398

Generation and diagnostics of pulsed intense ion beams with an energy density of 10 J/cm²

Yu. Isakova,[1,a)] A. Pushkarev,[1] I. Khailov,[1] and H. Zhong[2,b)]

[1]*Tomsk Polytechnic University, 30, Lenin Ave., 634050 Tomsk, Russia*
[2]*Beihang University, Beijing 100191, China*

The paper presents the results of a study on transportation and focusing of a pulsed ion beam at gigawatt power level, generated by a diode with explosive-emission cathode. The experiments were carried out with the TEMP-4M accelerator operating in double-pulse mode: the first pulse is of negative polarity (500 ns, 100-150 kV), and this is followed by a second pulse of positive polarity (120 ns, 200-250 kV). To reduce the beam divergence, we modified the construction of the diode. The width of the anode was increased compared to that of the cathode. We studied different configurations of planar and focusing strip diodes. It was found that the divergence of the ion beam formed by a planar strip diode, after construction modification, does not exceed 3° (half-angle). Modification to the construction of a focusing diode made it possible to reduce the beam divergence from 8° to 4°-5°, as well as to increase the energy density at the focus up to 10-12 J/cm², and decrease the shot to shot variation in the energy density from 10%-15% to 5%-6%. When measuring the ion beam energy density above the ablation threshold of the target material (3.5-4 J/cm²), we used a metal mesh with 50% transparency to lower the energy density. The influence of the metal mesh on beam transport has been studied. © 2015 AIP Publishing LLC. [http://dx.doi.org/10.1063/1.4926564]

I. INTRODUCTION

Pulsed ion beams (PIB) with energy densities of 1-10 J/cm² and the pulse duration of less than 100-200 ns provide intense heating and cooling of the near-surface layers of irradiated targets with a rate of more than 10^9 K/s. The pressure developed on the target is of the order of 10^7–10^{10} Pa.[1] Typical thickness of such a layer is 1-10 μm. This allows compounds and structures to be realized in surface layers which cannot be made by traditional industrial methods. The modifications can be extended into a depth of hundreds μm far beyond the typical ion range of 0.1–10 μm for ions of hundreds keV. As a result, the characteristics of materials change: solidity, strength, and wear resistance; therefore, the operational characteristics of items made from these materials improve.

For modification of materials with high-infrared conductivity, we need to use PIB with an energy density higher than 1–2 J/cm² and pulse duration of less than 100–150 ns. It is possible to obtain a high energy density on the target by focusing of the ion beam and eliminating beam scattering during transport. In ion diodes, geometric (ballistic) focusing is commonly used. Geometric focusing is achieved by curvature shape of the anode and cathode. However, while ions are propagated to the focus, their deviation from the initial path occurs due to Coulomb repulsion, influence of electromagnetic fields, diffusive scattering, etc.[2]

Several authors[3–7] analyzed propagation and focusing issues of pulsed ion beams. It was shown that magnetically insulated diodes exhibit a smaller ion beam divergence (ratio of the beam radius at half-height to the distance from the diode),

typically amounting to 1°–4°, in contrast to reflex diodes and pinch-diodes. PIB focusing properties are mainly affected by heterogeneous surface of the anode plasma, distortion of the electric field near the cathode, and the presence of magnetic field in the beam transport area, which makes difficult to keep the neutralizing electrons within the beam volume.

In our previous study,[8] we presented the results on transportation of PIB formed by a self-magnetically insulated diode with an explosive-emission cathode. The experiments have been performed using the TEMP-4M ion accelerator (200-250 kV, 120 ns). For increasing ion beam focusing efficiency and preventing the ion loss from the beam volume during propagation to the target, we used a metal shield installed on the grounded electrode. The shield was made from 1 mm stainless steel foil. Investigations were performed using a strip focusing diode, a cone diode, and a spiral diode with metal shields of different constructions. We observed that the beam diameter at the focus decreases from 60 mm (without shield) to 40–42 mm (with a shield) which leads to an increase in the energy density by a factor of 1.5–2 being 3–4 J/cm² at the focus. It was showed that use of a metal shield improves the transportation properties of PIB by keeping neutralizing electrons within the beam volume which ensures its space charge neutralization during the transport. According to the literature, defocusing of the beam in diodes with self-magnetic insulation is mainly affected by the configuration of the A-C gap. The aim of this paper is to design and experimentally validate the optimum construction of the diode which allows for reduction in the divergence of the ion beam.

II. EXPERIMENTAL SETUP

The experiments have been conducted using the TEMP-4M pulsed ion accelerator[9] which consists of the Marx

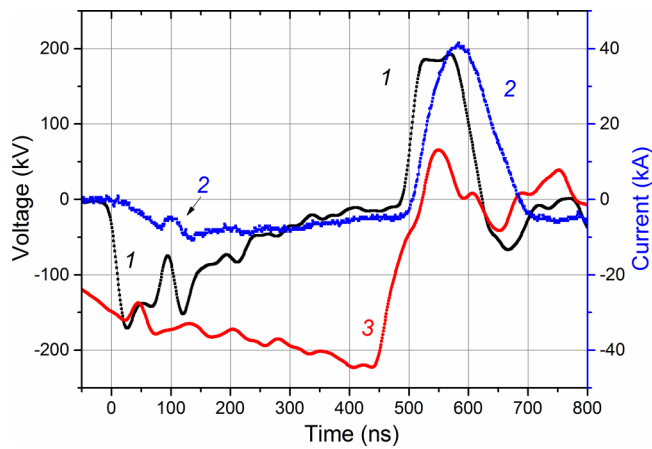a)E-mail: isakova_yulia@tpu.ru
b)E-mail: zhonghaowen@buaa.edu.cn

FIG. 1. Waveforms of voltage applied to the diode (1), total diode current (2), and charging voltage of Blumlein (3).

FIG. 3. Ion beam energy density distribution in the vertical cross section. These different curves are the energy density distribution obtained for five consecutive shots.

generator, double pulse transmission line (Blumlein), and vacuum ion diode with self-magnetic insulation of electrons. The accelerator configured in bipolar pulse operation mode forms two pulses of opposite polarity: the first pulse is of negative polarity (500 ns, 100-150 kV), and this is followed by a second pulse of positive polarity (120 ns, 200-250 kV). The ion beam energy density is 0.5-10 J/cm^2 (for different diode geometries), and pulse repetition rate is 5–10 pulses/min. Information on the diode connection, diagnostic equipment used in the TEMP-4M accelerator, and calibration can be found in our previous papers.[9,10] Typical waveforms are shown in Fig. 1.

To improve the reproducibility of the accelerating voltage pulse, the first voltage pulse at the output of Blumlein was used to trigger the main spark gap. The trigatron-type regime of the main spark gap operation showed a good stability of breakdown voltage and thus allowed to stabilize the duration of the first pulse.[11] The standard deviation of the breakdown voltage and duration of the first pulse did not exceed 2% for a set of 50 pulses.
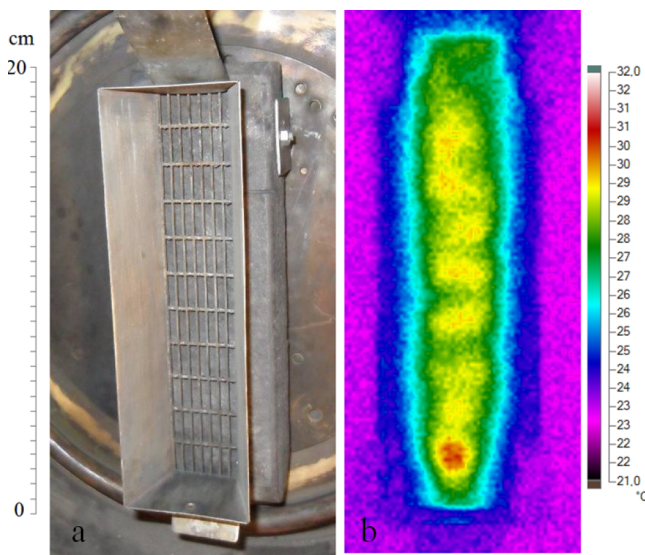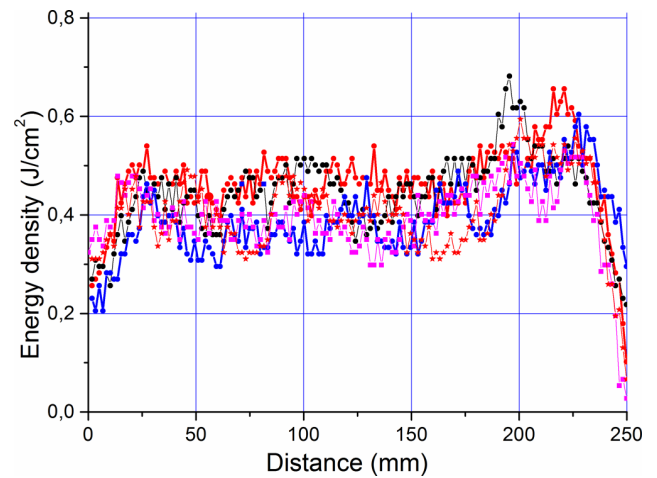
The majority of experiments were done using a strip focusing diode, measuring 22 cm × 4.5 cm, with the focusing distance being 14 cm. The A-C gap spacing of 8-9 mm was chosen so that diode impedance matches the characteristic wave impedance of Blumlein (4.9 Ohm). The potential electrode is made from graphite and the grounded electrode is made from stainless steel with a matrix of 2 cm × 0.5 cm slots for beam extraction, resulting in an overall transparency of 70%. The focusing diode has concave shaped electrodes focusing the beam within the yz plane, where the z-axis is in the beam propagation direction.

The voltage at the output of Blumlein was measured by a high-frequency high-voltage divider, which was installed in front of the diode connection. The total current in the diode was measured using a Rogowski coil.[10] The electrical signals coming from the sensors were recorded with a Tektronix 2024B oscilloscope (250 MHz, 5 GSPS). The ion beam parameters were measured using both a magnetically insulated Faraday cup ($B = 0.4$ T) for current density measurement and infrared imaging diagnostic for energy density measurement.[12] All studied diode geometries with graphite explosive emission cathodes worked effectively with the pressure in a diode chamber of 0.1 Pa and had an operational lifetime of up to 10^6 shots. Pulse repetition rate (5-6 pulses/min) was limited only due to heating of the diode and spark-gaps.

III. REDUCING DIVERGENCE OF AN ION BEAM

Analysis of literature showed that in ion diodes with self-magnetic insulation, the beam divergence can be reduced to 2°-3°. To improve beam focusing, we installed a solid metal

FIG. 2. Photograph of the strip planar diode and an infrared image of the beam. The length of the graphite electrode is 22 cm.
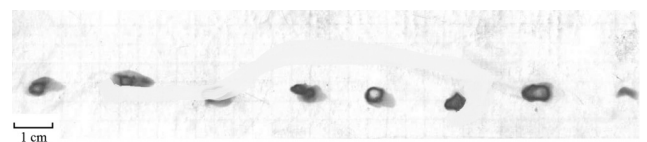

FIG. 4. Ion beam imprints on heat-sensitive paper. Obtained using a 2 mm pin-hole camera. Three consecutive shots.
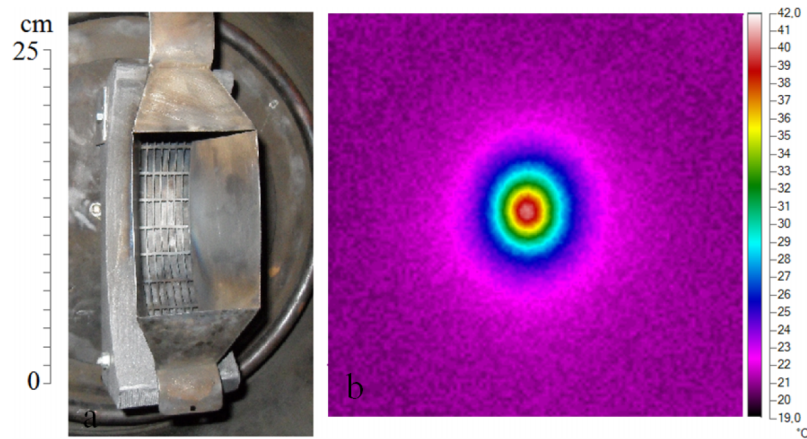
FIG. 5. Photograph of the strip focusing diode and an infrared image of the beam.

shield on the cathode.[8] The deviation angle and hence the total divergence angle have been significantly reduced from 11° to 8°-9° after installation of the shield. In the diode with self-magnetic insulation, used in our experiments, the cathode is designed as a strip measuring 22 cm × 4.5 cm, which is connected to the body of the diode chamber at one end only. In previous diodes' constructions, the width of the cathode and the anode was the same. But for formation of magnetic field in the A-C gap with a higher level of induction, a narrow strip cathode is needed, while the anode can be much wider to reduce distortion of electric field in the gap.

A. Planar strip diode

In order to reduce beam divergence in the planar strip diode, the anode of the diode was made from graphite with the length of 24 cm and the width of 8 cm. The cathode was 22 cm in length and 4.5 cm in width. Fig. 2 shows a photograph of the strip planar diode and an infrared image of the beam imprint on the target, obtained using infrared imaging diagnostics.

Temperature scale shown in Figs. 2, 5, and 9 is underestimated, since the IR camera records the temperature on the target through the CaF_2 window, which has a non-uniform transmittance in the wavelength range from 7 to 14 μm. To obtain real temperature values on the target, IR camera reading should be calibrated using the calibration dependence T_{real}

$= -47 + 3.52 \cdot T_{IR}$. Detailed information about the calibration procedure can be found elsewhere.[13]

A change made in the diode configuration resulted in improvement in the uniformity of the beam energy density distribution over cross section as well as it improved shot-to-shot reproducibility. Fig. 3 shows the distribution of energy density in vertical cross section.

Figure 4 shows the beam imprints on heat-sensitive paper obtained using a 2 mm pin-hole camera, which was located at 50 mm downstream from the diode. The diameter of the beam imprint was found to be 4-5 mm (Fig. 4).

Our measurements showed that the divergence of ion beam in transportation region does not exceed 3° (half-angle).

B. Focusing strip diode

Increase in the width of the anode in the focusing diode allowed for significant improvement in focusing properties. Fig. 5 shows the photograph of the focusing diode with the shield installed on the grounded electrode.

The width of the cathode was 4.5 cm, and the anode had a width of 9 cm. Modification of the diode constriction allowed to reduce the divergence angle from 8° to 4°-5° and increase the energy density at the focus of up to 10-12 J/cm², see Fig. 6.

Change in the diode design also increased the shot-to-shot reproducibility of the total diode current and energy density.
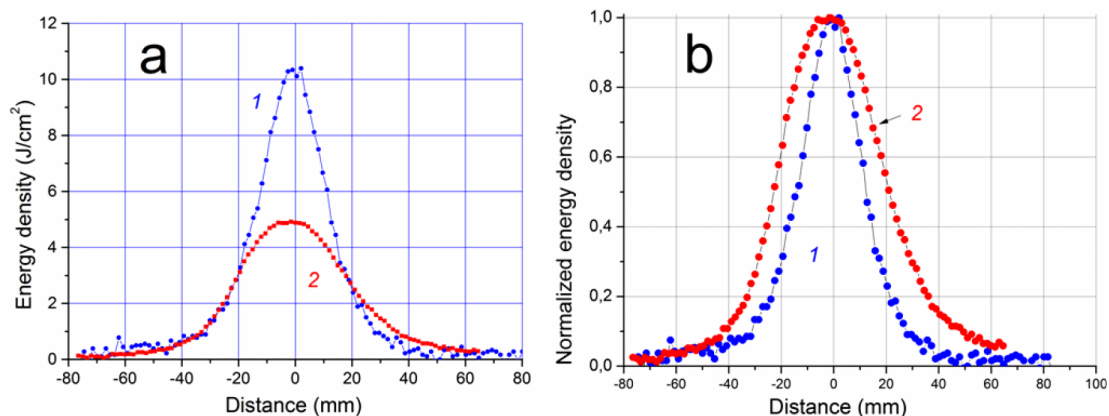

FIG. 6. Distribution of the beam energy density in the focal plane in vertical cross section with wide (1) and narrow (2) anodes. Absolute (a) and normalized (b) energy density.
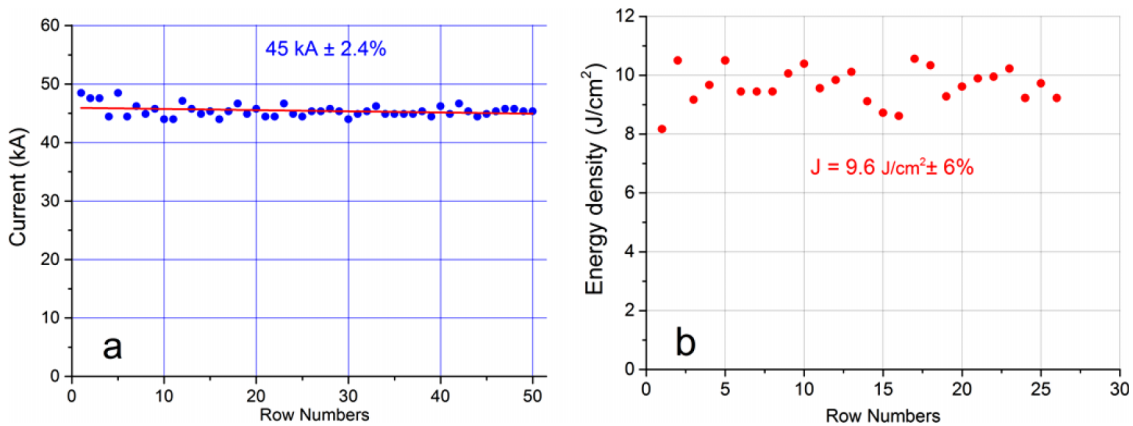
FIG. 7. Shot-to-shot variation in total diode current (a) and the beam energy density at the focus (b).

Figure 7 shows the results of statistical measurements. The pulse repetition frequency, when measuring total current, was 6 pulses/min, and when measuring energy density, 1 pulse in 2 min.

The standard deviation of the energy density decreased from 10%-15%[14] to 6%-7% and the same variation in total current decreased from 5%-6% to 2%-3%.

Modification in the diode configuration did not affect the diode operation mode; the impedance remained the same. Fig. 8 shows typical waveform of the accelerating voltage, experimental, and calculated impedance of the diode.

Taking into account the reduction of A-C spacing due to plasma expansion, the diode impedance is[15]

$$R_{calc} = \frac{U}{I_e} = \frac{(d_0 - v \cdot t)^2}{2.33 \times 10^{-6} \cdot S \cdot U^{1/2}},$$

where U is the voltage applied to the diode, d_0 is the initial (geometric) A-C gap spacing, S is the working surface area of the diode, and v is the plasma expansion speed (1.3 cm/μs).

C. Energy density measurement when ablation of the target takes place

To measure the ion beam energy density, we used infrared imaging diagnostics that measure the energy of the beam absorbed by the target.[12] However, when the beam energy density exceeds the ablation threshold of the target, the energy absorbed by the target is less than the incident energy, because some energy is carried away in the ablated material. This leads to an underestimation of the beam energy density when measured by infrared imaging diagnostic. In Ref. 16, authors used a metal mesh (transparency of 50%), intercepting the beam, while it propagates from the diode to target. Readings of infrared imaging diagnostics were then corrected taking into account optical transparency of the mesh. However, the transparency of the metal mesh can vary due to bridging the space between mesh wires by plasma. In Ref. 17, the authors observed underestimation of ion current density measurements by a Faraday cup due to closure of the collimating aperture by ablation plasma. Therefore, we performed testing of infrared diagnostics using a metal mesh with optical transparency of 50% (see Fig. 9).

Figure 10 shows the distribution of the energy density, formed by the focusing diode. Distance from the diode to target was 14 cm, and the distance from the diode to the metal mesh was 5 cm.

The energy density at the focus and the energy density distribution, calculated taking into account the optical transparency (50% and 25%) of the mesh, coincide well (within the accuracy of measurement).

Experiments showed that the metal mesh used for the attenuation of the ion beam may affect its divergence. When placing the mesh at the high energy density area (near focal point of the diode), the beam width at half-maximum decreases. Figure 11 shows the distribution of energy density formed by a focusing diode.
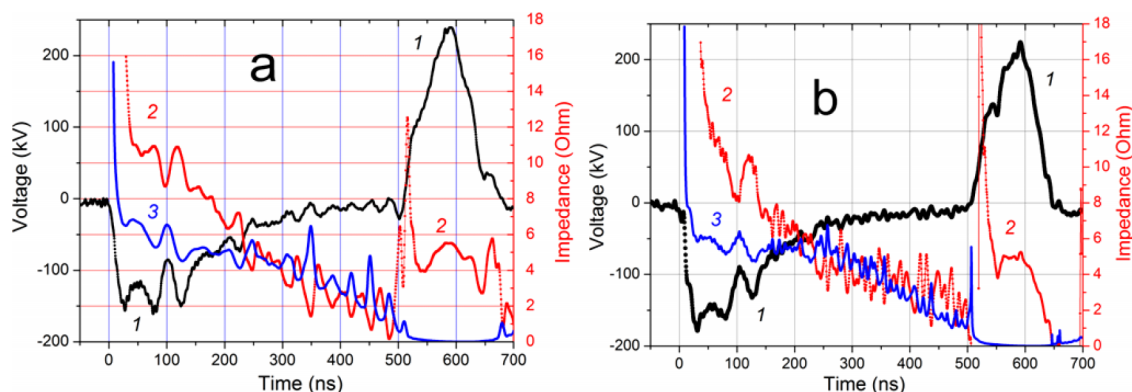

FIG. 8. Waveforms of accelerating voltage (1) and diode impedance (2—experiment; 3—calculation) for the focusing strip diode with a narrow (a) and wide (b) anode and the A-C spacing of gap 8 mm.
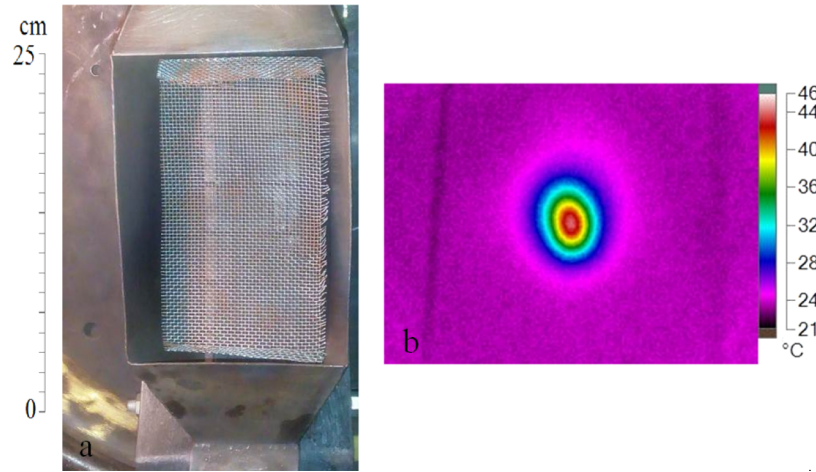
FIG. 9. Photograph of the strip focusing diode with metal mesh installed at the output of the focusing diode and an infrared image of the beam. Distance diode-target was 14 cm. The mesh was located 5 cm downstream from the cathode.
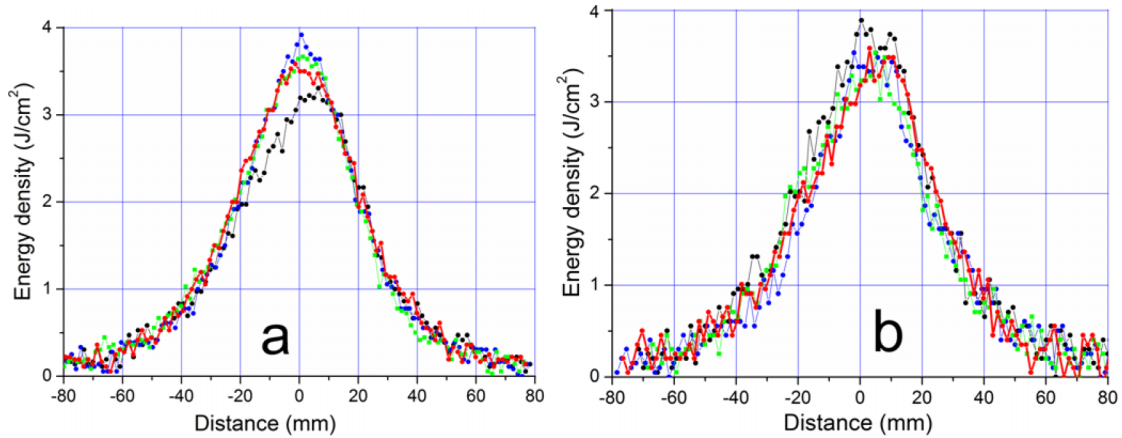

FIG. 10. Energy density distribution of the ion beam formed by the focusing diode, when using one mesh (a) and two meshes (b). Data for four consecutive pulses.
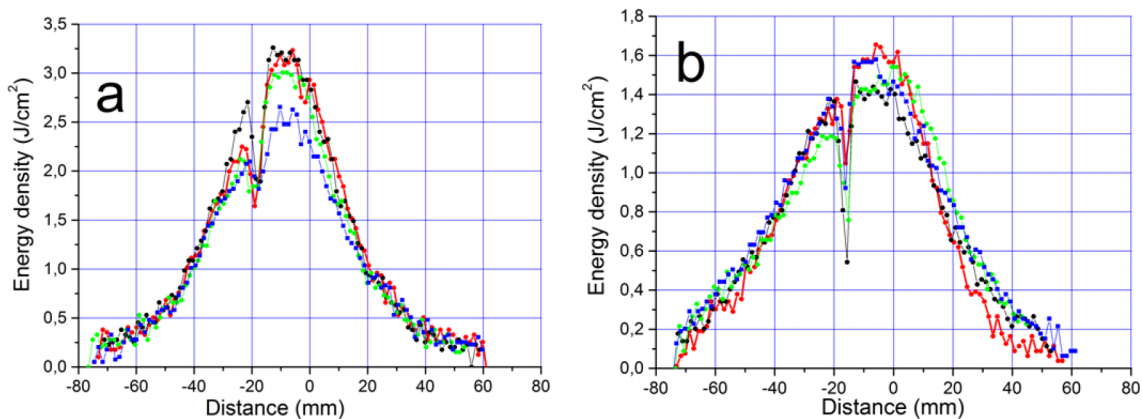

FIG. 11. Ion beam energy density distribution in vertical cross section, measured when using one mesh (a) two meshes (b). Data for four consecutive pulses.

The distance from the diode to target was 19.5 cm while the distance from the diode to the mesh was 10 cm (diode focusing distance is 14 cm). To combine the energy density patterns obtained at different shots, we made 3 mm diameter hole in the target (see Fig. 11).

With high energy density in the region nearby the metal mesh, an additional focusing of the beam may occur, and its width (at half-height) is reduced from 60 mm to 50-55 mm. The energy density increases.

D. Calculation of the threshold energy density

At the melting point of iron being 1800 K, density of 7.8 g/cm^3, heat capacity of 0.65 J/(g·°C), and the specific heat
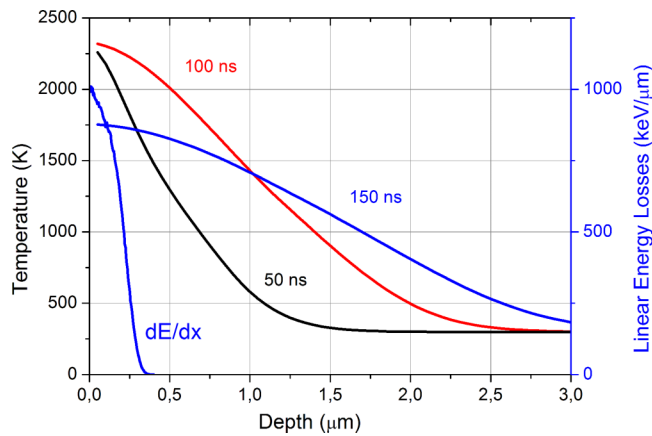
FIG. 12. Linear energy losses of C^+ ions and temperature distribution in stainless steel target irradiated with ion beam at different times after interception with the beam.
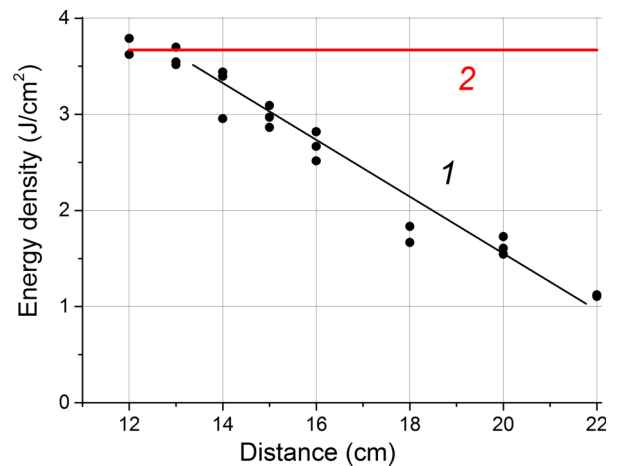

FIG. 13. Dependence of the maximum energy density on the distance diode-target (1) and calculated minimum energy density required for evaporation of the target material (2).

of fusion of 277 J/g, the volume density of energy deposited in target, required for melting, is 7 kJ/cm^3. Ion beam, formed by a diode with a graphite anode, is mainly composed of carbon ions (70%-80%) and protons. Figure 12 shows the results of simulation of the temperature distribution along the depth for a stainless steel target irradiated with ions C^+ and protons (70% C^+ + 30% H^+) having the energy of 200 keV at different times after interception with the beam.

The simulation was made using the Comsol Multiphysics program for the following parameters: pulse duration of 100 ns, Gaussian pulse shape, and ion beam energy density of 1 J/cm^2. Phase transformation was not taken into account. The simulation results show that with ion range being less than 0.3 μm, the thermal field front expands to 2 μm depth by the end of the pulse. When calculating the surface energy density, we took into account not the range of ions in the target but the depth of the thermal field propagation. The results of calculation of the beam energy density, sufficient for melting and vaporization of the surface layer of a target made from stainless steel, are shown in Table I.

The calculation was performed for heat capacity of liquid steel being 0.83 J/(g·°C). Fig. 13 shows the results of measurement of the beam energy density, obtained at different distances from diode to target.

Our observation shows that the maximum energy density, measured with the infrared imaging diagnostics (without mesh), coincides with the calculation of evaporation threshold stainless steel target (see Table I).

IV. CONCLUSION

Our studies showed that the divergence of a pulsed ion beam generated in the diode with self-magnetic insulation largely depends on the uniformity of electric field in the A-C gap. The distortion of the electric field at the diode edge increases beam divergence during transportation. To reduce the beam divergence, we modified the construction of the diode. The width of the anode was increased compared to that of the cathode. Change in the diode construction did not affect the operation of the diode and its impedance remained the same. We observed that the divergence of the beam formed by a planar strip diode was reduced to 3° (half-angle). Modification to the construction of a focusing diode made it possible to reduce the beam divergence from 8° to 4°-5°, as well as to increase the energy density at the focus up to 10-12 J/cm^2, and decrease the shot-to-shot variation in the energy density from 10%-15% to 5%-6%.

To measure the ion beam energy density, we used infrared imaging diagnostics that measure the energy of the beam absorbed by the target. However, when the beam energy density exceeds the ablation threshold of the target, the IR-diagnostics give underestimated values of the energy density. Experiments showed that the metal mesh used for the attenuation of the ion beam might cause significant errors in IR measurements. With the high energy density of the beam, the mesh placed near the diode focal point may affect the divergence of the beam. The energy density absorbed by the target, measured with IR diagnostics, can vary 1.5-2 times when using meshes even in the absence of the target ablation. Optimizing of the location of metal meshes in the beam transport-focusing area allows for eliminating this error.

The combination of a long service life of diodes with self-insulation and explosive-emission cathode (more than 10^6 pulses) and good shot-to-shot reproducibility makes these

TABLE I. Calculation of the ion beam energy density required for phase transition in a steel target.

		Mass density of deposited energy (J/g)	Volume density of deposited energy	Ion beam energy density (J/cm^2)
1	Transformation to a melting point 300-1800 K	975	7600 J/cm^3	1.52
2	Melting	277	2160 J/cm^3	0.43
3	Transformation to a boiling point 1800-3135 K	1100	8580 J/cm^3	1.72
			Phases 1-3 together	3.67

diodes the very promising for industrial applications where high-energy beams are used for the surface modification of materials.

[1]V. I. Boyko, V. A. Skvortsov, V. E. Fortov, and I. V. Shamanin, *The interaction of pulsed charged-particle beams with a substance* (Fizmatlit, Moscow, 2003), p. 286 [in Russian].

[2]S. Humphries, *Charged Particle Beam* (Wiley, New York, 1990), p. 847.

[3]C. L. Olson, "Ion beam propagation and focusing," J. Fusion Energy **1**(4), 309–339 (1982).

[4]K. Yatsui, A. Tokuchi, H. Tanaka, H. Ishizuka, A. Kawai, E. Sai, K. Masugata, M. Ito, and M. Matsui, "Geometric focusing of intense pulsed ion beams from racetrack type magnetically insulated diodes," Laser Part. Beams **3**(2), 119–155 (1985).

[5]V. M. Bystritskii, Yu. A. Glushko, A. V. Kharlov, and A. A. Sinebryukhov, "Experiments on high power ion beam generation in self-insulated diodes," Laser Part. Beams **9**(3), 691–698 (1991).

[6]K. W. Zieher, "Investigation of a pulsed self-magnetically Bθ insulated ion diode," Nucl. Instrum. Methods Phys. Res. **228**, 161–168 (1984).

[7]K. W. Zieher, "Necessary condition for current neutralization of an ion beam propagating into vacuum from a self-magnetically Bθ-insulated ion diode," Nucl. Instrum. Methods **228**(1), 169–173 (1984).

[8]A. I. Pushkarev, Yu. I. Isakova, and I. P. Khailov, "The influence of a shield on intense ion beam transportation," Laser Part. Beams **31**(03), 493–501 (2013).

[9]A. I. Pushkarev and Yu. I. Isakova, "A gigawatt power pulsed ion beam generator for industrial application," Surf. Coat. Technol. **228**, 382–384 (2013).

[10]Y. I. Isakova, "Diagnostic equipment of the TEMP-4M pulsed ion beam generator," J. Korean Phys. Soc. **59**(6), 3531–3535 (2011).

[11]A. I. Pushkarev, Y. I. Isakova, and I. P. Khaylov, "Improvement in the statistical operation of a Blumlein pulse forming line in bipolar pulse mode," Rev. Sci. Instrum. **85**, 073303 (2014).

[12]Y. I. Isakova and A. I. Pushkarev, "Thermal imaging diagnostics of powerful ion beams," Instrum. Exp. Tech. **56**(2), 185–192 (2013).

[13]Y. I. Isakova, "Infrared imaging diagnostics for parameters of powerful ion beams formed by a diode in a double-pulse mode," in *Proceedings of Pulsed Power Conference (PPC)* (IEEE, 2011), pp. 334–340.

[14]Y. I. Isakova, A. I. Pushkarev, and I. P. Khaylov, "Statistical analysis of the ion beam production in a self magnetically insulated diode," Phys. Plasmas **20**(9), 093105 (2013).

[15]A. I. Pushkarev, Yu. I. Isakova, and V. I. Guselnikov, "Limitation of the electron emission in an ion diode with magnetic self-insulation," Phys. Plasmas **18**, 083109 (2011).

[16]H. A. Davis, R. R. Bartsch, J. C. Olson, D. J. Rej, and W. J. Waganaar, "Intense ion beam optimization and characterization with infrared imaging," J. Appl. Phys. **82**(7), 3223 (1997).

[17]T. J. Renk, V. Harper-Slaboszewicz, K. A. Mikkelson, W. C. Ginn, P. F. Ottinger, and J. W. Schumer, "Use of a radial self-field diode geometry for intense pulsed ion beam generation at 6 MeV on Hermes III," Phys. Plasmas **21**, 123114 (2014).